JOM, Vol. 71, No. 12, 2019
https://doi.org/10.1007/s11837-019-03740-0
© 2019 The Minerals, Metals & Materials Society

Extraction of Copper and Nickel from Low-Grade Nickel Sulfide Ore by Low-Temperature Roasting, Selective Decomposition and Water-Leaching Process

WENNING MU,[1,2,3,5] ZHIPENG HUANG,[1,3] HAIXIA XIN,[1,2,3] SHAOHUA LUO,[1,2,3] YUCHUN ZHAI,[2,3] and QIAN XU[4]

1.—School of Materials Science and Engineering, Northeastern University, Shenyang 110819, Liaoning, China. 2.—School of Resources and Materials, Northeastern University at Qinhuangdao, Qinhuangdao 066004, Heibei, China. 3.—Key Laboratory of Resources Cleaner Conversion and Efficient Utilization Qinhuangdao City, Qinhuangdao 066004, Heibei, China. 4.—School of Materials Science and Engineering, Shanghai University, Shanghai 200072, China. 5.—e-mail: muwn@neuq.edu.cn

Low-temperature roasting, selective decomposition and water-leaching were used to extract nickel and copper from low-grade nickel sulfide ore with highly alkaline gangue. The effects of variable factors, such as the dosage of roasting additives, the ore particle size, roasting time and roasting temperature, selective decomposition temperature and leaching temperature on the conversion of metals were investigated. The roasting process contained liquid–solid and gas–solid reactions, which were controlled by internal diffusion. X-ray diffraction analysis of the roasting clinkers presented that the metal sulfides were first converted into intermediate products of metallic ammonium sulfate salts or metal sulfate by reacting with ammonium sulfate, and finally formed stable metal-sodium double salts by the action of sodium sulfate. Proportions of 99.13% nickel and 96.74% copper can be effectively extracted, while 95.95% iron was removed by selectively decomposing iron-containing sulfates to form ferric oxide, or separating as natrojarosite in a water-leaching process.

INTRODUCTION

The Jinchuan Group (JNMC) is the largest producer of electrolytic nickel in China, mainly producing nickel, copper, cobalt and platinum group precious metals. It owns the Jinchuan nickel-copper mine, which is a world-famous super-large polymetallic symbiotic magmatic sulfide deposit with proven reserves of 520 million tons, containing approximately 5.5 million tons of nickel, 3.43 million tons of copper and 0.16 million tons of cobalt. The deposit has been formed by sulfide segregation from mantle-derived mafic–ultramafic magma;[1] the valuable metals such as Cu, Ni and platinum group elements are highly compatible in sulfides.[2] The sulfide nickel ore is processed by flotation to produce nickel concentrate, followed by high-temperature smelting and blowing to prepare high-nickel matte.[3] With nearly 60 years of exploitation, high-grade nickel sulfide resources are nearing depletion, and low-grade nickel sulfide ore has become JNMC's raw material to produce nickel.

Compared with high-grade nickel sulfide ores, low-grade nickel sulfide minerals have a lower nickel grade, higher gangue content, and more complex composition and structure. If this ore is treated with the existing nickel sulfide ore smelting process, a large number of valuable metals are lost in the flotation process,[4] coupled with high energy consumption caused by high-temperature operation, resulting in high costs and poor economic benefit of the entire smelting process.[5] Taking JNMC's concentrate with an annual output of 8 million tons as an example, when the traditional process is adopted to treat low-grade nickel sulfide ore with high alkaline gangue, about 15,000 tons of nickel and 20,000 tons of copper are lost during the process of beneficiation, nearly 5000 tons of nickel and

(Published online September 10, 2019)

1000 tons of cobalt are lost in the concentrate smelting process, and the economic loss caused by the loss of metal is nearly 3 billion yuan per year.

In order to obtain a higher concentrate grade and less loss of valuable metals, some studies on the improvement of the flotation process[6] and the development of new flotation reagents[7] have been carried out, but no breakthrough results have been achieved. Many researchers have begun to focus on directly extracting valuable metals from low-grade nickel sulfide ore by hydrometallurgical methods. Oxygen pressure sulfuric acid leaching is used to directly recover nickel, copper and cobalt from mechanically activated complex sulfide ore in the early stage, but the application of the process is limited by high-level equipment and high maintenance costs.[8] Mixed nitric-sulfuric acid leaching at ambient temperature and atmospheric pressure is proposed to deal with low-grade Ni-Cu sulfide tailings, although excellent recovery yields of nickel, copper and cobalt can be achieved, while a too long reaction time results in poor production efficiency.[9] Heap bioleaching[10] and column bioleaching[11,12] has been widely studied for processing low-grade nickel sulfide ore; the high content alkaline gangue in the ores leads to high acid consumption, long leaching time and low efficiency.[13,14] A staged leaching process is suggested to treat complex polymetallic sulfide concentrates, although some valuable metals including Au, Ag, Cu, Zn and Pb can be effectively extracted, the long process and complicated operation has restricted further development of the technology.[15] Thus, it is very necessary to develop a new and clean process to directly extract valuable metals from low-grade nickel sulfide ore.

In this work, low-temperature roasting, selective decomposition and a water-leaching process are proposed to extract nickel and copper from Jinchuan low-grade nickel sulfide with highly alkaline gangue. The effects of roasting additive dosage, ore particle size, roasting time and roasting temperature on metal conversions have been studied in detail in the low-temperature roasting process from an experimental perspective, and by micro-morphology and phase conversion. Several kinetics models have been utilized to analyze the kinetics of the roasting process to obtain a process control step and kinetics equation. The selective decomposition temperature and leaching temperature were optimized to remove iron. XRD, SEM and EDS were used to analyze the phase composition and microstructure of solid samples to reveal the roasting reaction mechanism.

EXPERIMENTAL

Materials and Reagents

The low-grade nickel sulfide ore used in this research was provided by JNMC, Gansu province, China. The ore samples were crushed, ground and sieved to yield a particle size of − 20 mesh after drying at 80°C for 12 h. The reaction reagents, including ammonium sulfate and sodium sulfate, were analytical grade supplied by the Tianjin Chemical Reagent plant (China). Purified water was used throughout all the experiments.

The chemical analysis of the ore samples is given in Table I, from which it can be seen that 4.63% Ni and 2.75% Cu are present as major valuable metals, while the other metals include Fe and Mg at 32.23% and 7.24%, respectively. The major mineral phases within the ore, which is indicated from the XRD (Rint-2000, Rigaku) pattern in Fig. 1a, are talc ($Mg_3Si_4O_{10}(OH)_2$), lizardite ($Mg_3Si_2O_5(OH)_4$), pyrite (FeS_2), pyrrhotite (Fe_7S_8), magnetite (Fe_3O_4), chalcopyrite ($CuFeS_2$) and pentlandite ($Fe_9Ni_9S_{16}$).

The particle morphology and surface composition of the ore samples were analyzed using SEM and EDS (Leo Supra 35, Germany), and the results are shown in Fig. 1b–j. Figure 1b shows that the ore powders have irregular shapes, are laminated and have a loose surface. The gangue is mainly lizardite and talc, which have a fine-grained fibrous or leaf-shaped structure and are symbiotically intermingled in the ore. The structure in the blue boxed area shows that gangue accounts for a considerable proportion of the ore composition. The EDS elemental maps of the ore samples in Fig. 1c–j show that the elements of O, Mg and Si have similar aggregated states forming talc and lizardite; the elements of Fe, S and Cu have similar distributions constituting chalcopyrite and pyrite.

Methods and Procedure

Low-Temperature Roasting Process

The dried ore powders of 10-g scale were thoroughly mixed with ammonium sulfate and sodium sulfate at a predetermined mass ratio (MR). The mixture was placed in a ceramic crucible, put into a shaft furnace equipped with a bottom gas inlet device and a top offgas absorption device, and roasted at different temperatures varying from 400°C to 500°C for a period of time. Subsequently, the furnace was naturally cooled to room temperature to obtain clinkers.

Selective Decomposition Process

The clinkers obtained from the low-temperature roasting process were heated at a temperature range of 480–750°C for a preset time. The soluble metal sulfates in the clinkers can be selectively decomposed by controlling the roasting temperature and roasting time. After cooling, high-temperature roasted clinkers were obtained.

Water-Leaching Process

The roasted clinkers were leached with purified water in a water bath. Unless otherwise stated, the leaching conditions were fixed with a liquid-to-solid ratio of 5:1 (mL:g), leaching time of 1 h, a stirring

Table I. The main chemical compositions of low-grade nickel sulfide ore

Composition	S	Ni	TFe	Cu	Mg	SiO_2	Al_2O_3	CaO	Other
wt.%	21.50	4.63	32.23	2.75	7.24	16.12	0.90	1.22	13.41

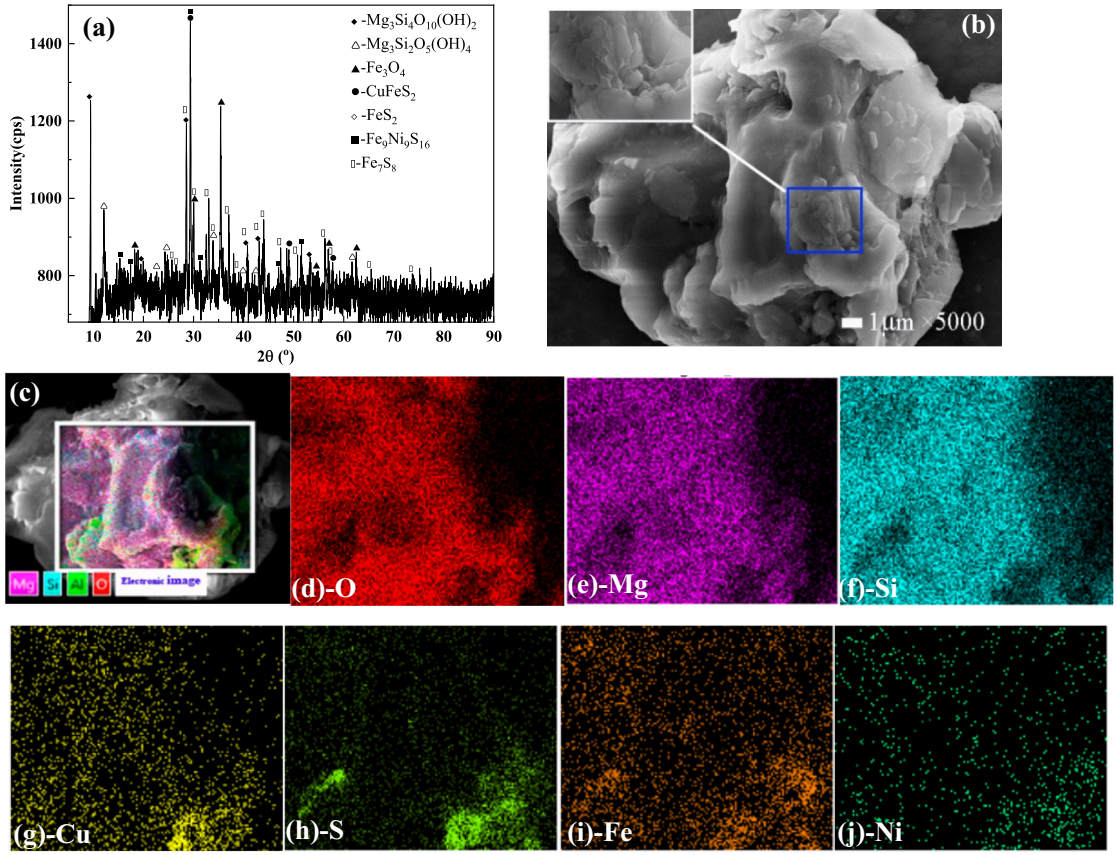

Fig. 1. XRD patterns (a), SEM images (b) and EDS elemental maps (c–j) of low-grade nickel sulfide ore.

speed of 300 rpm and a leaching temperature of 80°C. Filtration was carried out to collect the leaching solution, and the solid residues were washed thoroughly several times with purified water and dried for XRD and SEM analysis. The concentrations of metal ions in the leaching solution and the washing liquid were determined according to standard chemical titration (iron and magnesium) and UV–Vis spectrophotometry (copper and nickel), and the conversion of various metals can be calculated from Eq. 1. The flow chart of extracting nickel and copper from low-grade nickel sulfide ore is shown in Fig. 2.

$$\alpha_i = \frac{c_i V_i}{w_i m} \times 100\% \quad (1)$$

where α_i (%) is the conversion of the metal elements, c_i (g/L) is the concentration of metal ions in the mixed solution of the leaching solution and the washing solution, V_i (L) is the volume of the leaching solution, w_i (wt.%) is the content of metal elements in the ore, and m (g) is the mass of the ore powders used in the roasting procedure.

RESULTS AND DISCUSSION

Low-Temperature Roasting Process

In order to investigate the effects of additive dosage, particle size of the ore sample, and roasting temperature and time on the conversion of nickel, copper, iron and magnesium in the low-temperature roasting process, the ore samples roasted under different conditions were directly subjected to a water-leaching process, and the leaching solution was collected to determine the metal content and calculate the metal conversion.

Effect of Roasting Additive Dosage

Ammonium sulfate was used as the main roasting agent due to its high reactivity and ease of

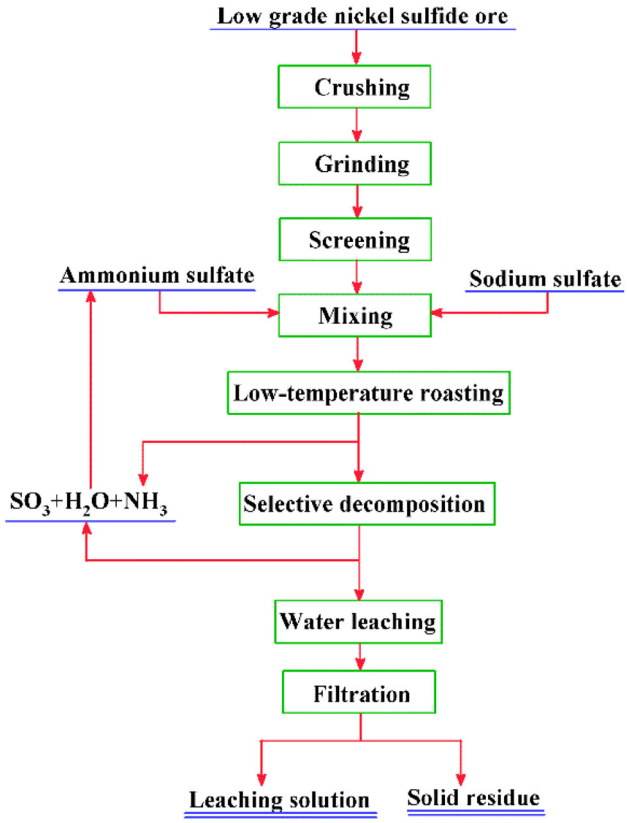

Fig. 2. Flow chart of extracting nickel and copper from low-grade nickel sulfide ore.

recovery,[16–18] and sodium sulfate was chosen as a catalyst to enhance the conversion of the metals.[19] In order to determine the dosage of additives, the ore with a particle size of − 160 + 180 mesh were mixed with sodium sulfate and ammonium sulfate at a MR of 1:x:y (x = 0, 0.1, 0.2, 0.3, 0.35, 0.4, 0.45, 0.5; y = 0, 1, 2, 3, 3.5, 4), and roasted at 450°C for 120 min, and the relationship between the conversion of metals and the dosage of additives is shown in Fig. 3.

Figure 3a shows that 70.36% nickel, 64.16% copper, 40.51% iron and 24.14% magnesium is extracted when x is 0; the result of the reaction between ammonium sulfate and the metals. With the increase of the sodium sulfate dosage, the conversion of nickel and copper increases gradually to the maxima of 93.48% and 92.58% (x = 0.4), which are increased by 23.12% and 28.61%, respectively, compared with no sodium sulfate added. As the sodium sulfate dosage is further increased, the conversion of copper and nickel decreases. The iron conversion is most affected by the addition of sodium sulfate. When x is only 0.1, it has been increased by approximately 40%, and then slowly increases with the increase of x until the maximum iron conversion of 80.71% is reached (x = 0.3), then the curve shows a decreasing trend. Magnesium conversion increases with the dosage of sodium sulfate, but the maximum conversion is less than 60%.

Figure 3b shows that the conversions of nickel, copper, iron and magnesium increase significantly with the increase of ammonium sulfate dosage (y) from 1 to 3.5. When $y > 3.5$, the conversion curves of metals tend to be flat. The reaction of ammonium sulfate with the ore is the main reaction in the roasting system. According to theoretical calculations, the ammonium sulfate dosage (y) required for the complete reaction of all metal components is about 1.6. In the roasting experiments, an excessive ammonium sulfate dosage is required to ensure sufficient contact with the ore powders; y = 3.5 is a suitable ammonium sulfate dosage.

The XRD patterns of the clinkers and the leaching residue are shown in Fig. 3d. When x = 0, the diffraction peaks labeled 1, 2, 3 and 4 are intense, indicating that the nickel, iron and copper components have reacted with the ammonium sulfate to produce metallic ammonium sulfate salts and metal sulfates. When sodium sulfate is added (x = 0.2), the diffraction peaks of the metallic ammonium sulfate salts are enhanced, and diffraction peaks of the metal-sodium double salts (labeled 6, 7, 8, and 9) appear. When x = 0.4, the diffraction peaks of the metallic ammonium sulfate salts disappear, while the diffraction peaks of the metal-sodium double salts are significantly enhanced, especially the diffraction peaks of $NaMgFe(SO_4)_3$. This indicates that the metallic ammonium sulfate salts can react with sodium sulfate to convert into soluble metal-sodium double salts. The diffraction peaks of talc, labeled 5, are always weakened, indicating that the magnesium conversion is effectively improved under the action of sodium sulfate.

The trivalent iron ion (Fe^{3+}) is relatively unstable in the water-leaching process, which can form insoluble natrojarosite ($NaFe_3(SO_4)_2(OH)_6$) according to Eq. 2.[19] Part of the iron-bearing sulfates can be decomposed into ferric oxide remaining in the residue together with natrojarosite. The reduction of the iron concentration in the leaching solution leads to the decrease of iron conversion. The XRD analysis of the residue in Fig. 3d demonstrates the formation of ferric oxide and natrojarosite.

$$3Fe^{3+} + Na^{+} + 2SO_4^{2-} + 6H_2O = NaFe_3(SO_4)_2(OH)_6 + 6H^{+} \quad (2)$$

The SEM images in Fig. 4a show that the clinker exhibits a loose, porous and multi-layered sheet structure when x = 0, and the roasting system contains solid–solid–gas reaction. When sodium sulfate (x = 0.2) is added, the particles of the clinker stick together and a porous structure, shown in Fig. 4b, demonstrates the generation of a liquid phase. When the dosage of sodium sulfate is increased to x = 0.4, the increase of the liquid Na-pyrosulfate produced by the reaction of sodium sulfate with SO_3 released through the

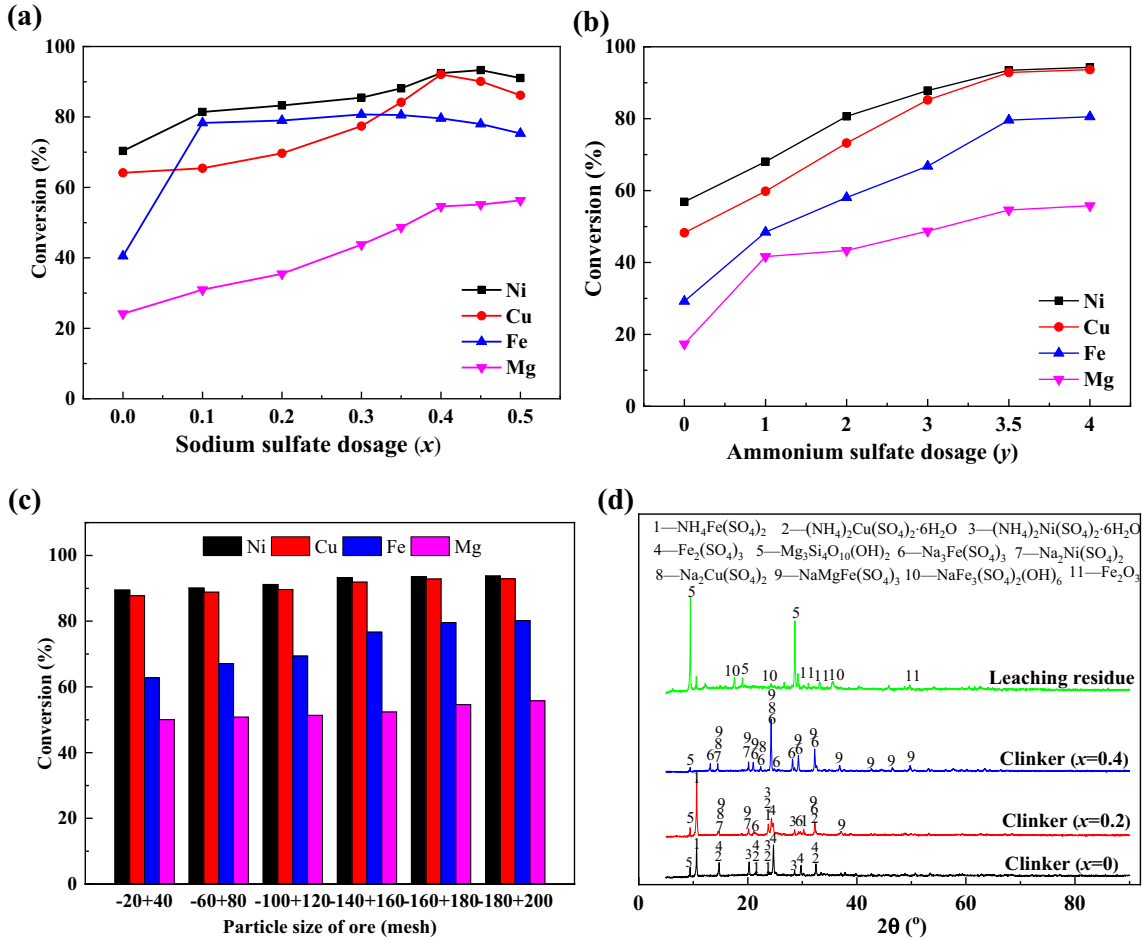

Fig. 3. The effect of the following factors on the conversion of metals and the XRD patterns of clinkers and the leaching residue, (a) sodium sulfate dosage, y = 3.5; (b) ammonium sulfate dosage, x = 0.4; (c) the particle size of the ore; (d) XRD patterns.

decomposition of ammonium sulfate causes an increase in the corrosion degree of the ore, and the ore structure is completely disintegrated to form deep pores and a large void morphology, while some small particles are bonded together, as seen in Fig. 4c. As the sodium sulfate dosage is increased further, the degree of particle adhesion increases and the mass transfer within the system is hindered, which leads to the decrease in the conversion of nickel and copper when $x > 0.4$. The most favorable sodium sulfate dosage (x) of 0.4 was chosen for the roasting process.

Effect of Ore Particle Size

The effects of the ore particle size on the conversion of the metals were conducted under the following conditions: roasting temperature 450°C, roasting time 120 min, and MR 1:0.4:3.5.

As shown in Fig. 3c, the ore particle size has little effect on the conversion of the metals. When the ore particle size is decreased, the conversion of nickel, copper, and magnesium increases by less than 5%, while iron conversion increases by about 17%. When the particle size of ore is − 140 + 160 mesh, the conversions of nickel and copper are higher than 92%, and the further reduction of the ore particle size does not cause their significant increase. When the screen size is increased, the ore particle size decreases and the specific surface area increases, so that the effective reaction area of the ore powders is increased and the conversion of the metal components, especially iron, is improved.

The SEM images in Fig. 4d show that, when the ore fineness is large, the clinker size is large, the particles are not uniform, the shape is irregular, and a shallow layer structure is formed on the surface. As the ore particle size decreases, the clinker size decreases and gradually tends to be homogeneous, with a loose flower-like structure being formed on the surface due to the increase of reaction degree (Fig. 4e). When the ore particle size is too small, an agglomeration phenomenon can be observed on the clinker surface, with many small particles adhering to the large particles, as seen in Fig. 4f, which is disadvantageous for the roasting reaction. In order to obtain fine ore powders, the grinding time and energy consumption are increased. The appropriate particle size of

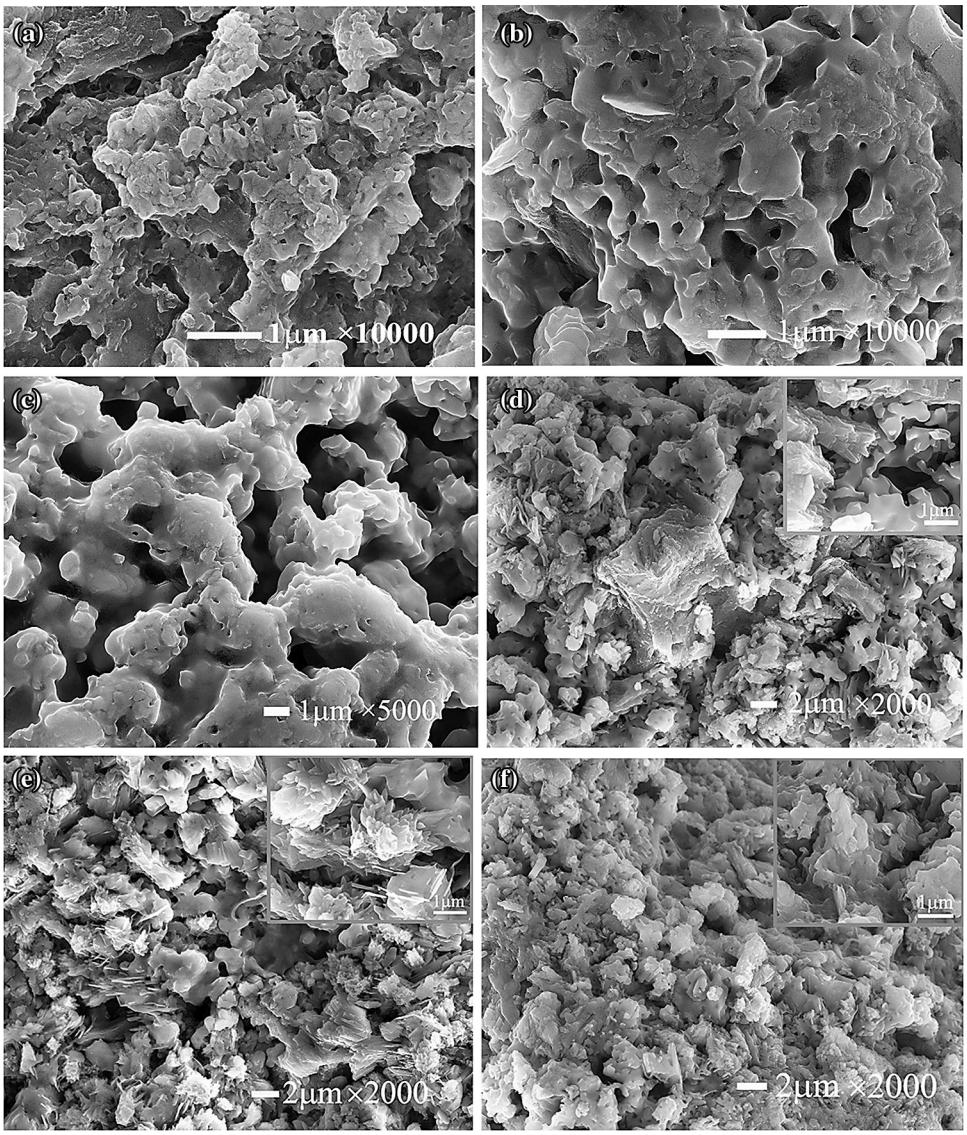

Fig. 4. The SEM image comparison of clinkers with different dosages of sodium sulfate, (a) x = 0; (b) x = 0.2; (c) x = 0.4 and for different sizes of roasted clinker, (d) − 20 + 40 mesh; (e) − 140 + 160 mesh; (f) − 200 mesh.

− 140 + 160 mesh was selected for the subsequent experiments.

Effect of Roasting Temperature and Time

The effect of roasting temperature and time on the conversion of metals was studied in the temperature range of 400–500°C and the roasting time range of 0–120 min. Other experimental conditions were fixed at a MR of 1:0.4:3.5 and a particle size of − 140 + 160 mesh.

Figure 5a–d indicates that the conversion of the metals first increases rapidly and then increases slowly with the increase of roasting time when the roasting temperature varies from 400°C to 450°C. Under the same roasting time, the conversion of nickel and copper can be effectively increased by increasing the roasting temperature, the magnesium conversion increases only slightly, and the iron conversion reaches a maximum of 79.9% at 450°C and then decreases at 500°C. This can be attributed to the decomposition of the iron–sodium double salt and ammonium ferric sulfate to form water-insoluble ferric oxide. When the roasting time is 120 min and the roasting temperature is 500°C, the conversion of nickel and copper can reach 93.2% and 95.4%, respectively.

Figure 5e presents the XRD pattern of clinkers obtained at different roasting temperatures. When the roasting temperature is below 350°C, the diffraction peaks of ammonium sulfate are obvious, and no new phase is produced, showing that the ore and ammonium sulfate have not reacted. When the roasting temperature is increased to 350°C, the diffraction peaks of ammonium pyrosulfate ($(NH_4)_2S_2O_7$), sodium dithionate ($Na_2S_2O_6{\cdot}2H_2O$) and Na-pyrosulfate ($Na_2S_2O_7$) labeled 2, 3, 4,

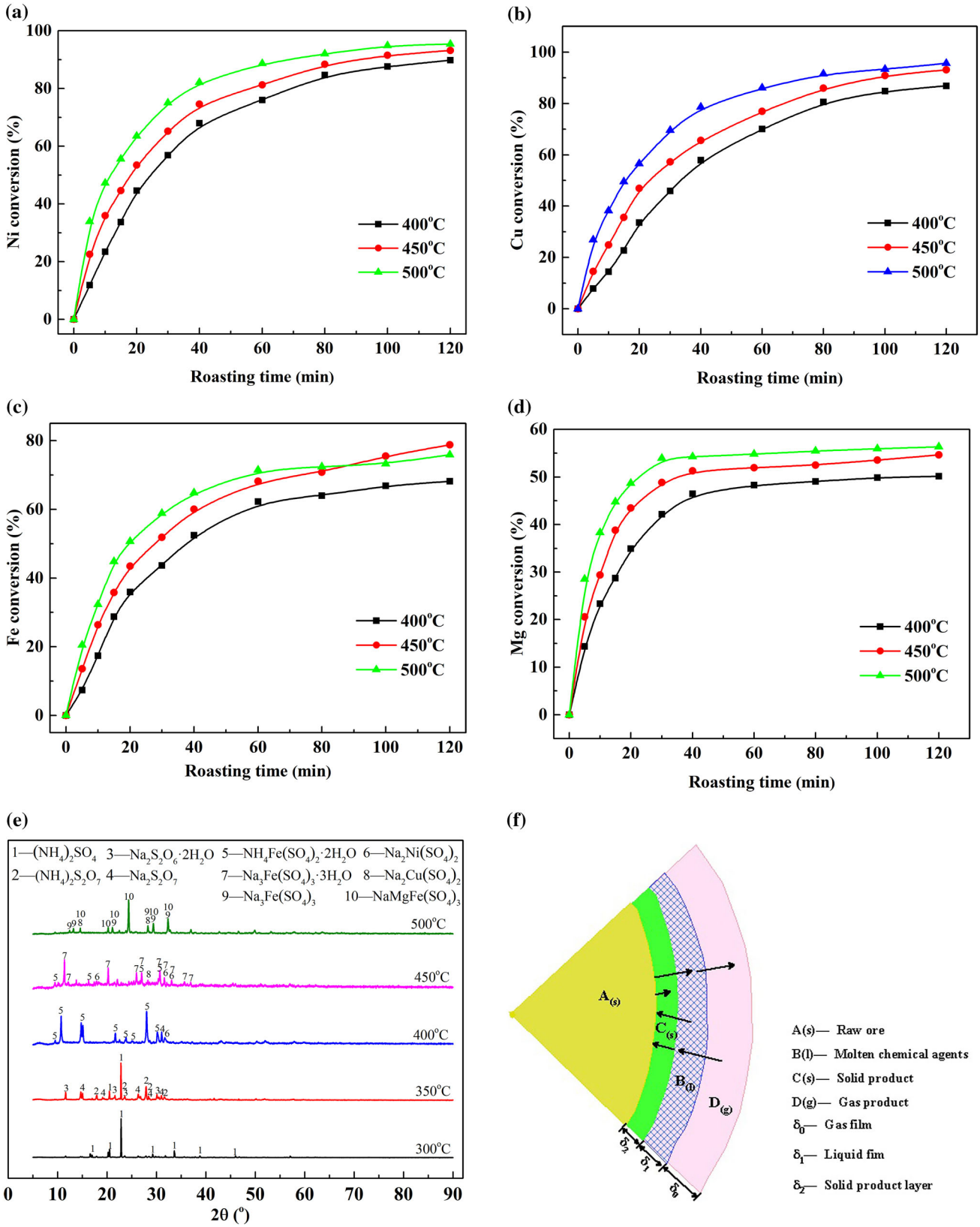

Fig. 5. Effect of roasting temperature and roasting time on the conversion of metals, XRD patterns of the clinkers and the reaction model of the roasting process, (a) Ni; (b) Cu; (c) Fe; (d) Mg; (e) XRD patterns; (f) reaction model.

appear. This indicates that ammonium sulfate has been decomposed, and the released SO_3 has reacted with sodium sulfate to form Na-pyrosulfate and sodium dithionate.

With the increase of roasting temperature, the diffraction peaks labeled 1, 2, 3, 4 gradually disappear. At 400°C, the obvious diffraction peaks of ammonium ferric sulfate appear. At 450°C, the diffraction peaks of $Na_2Cu(SO_4)_2$ and $Na_3Fe(SO_4)_3{\cdot}3H_2O$ appear, the diffraction peaks of $Na_2Ni(SO_4)_2$ are more obvious, and some diffraction peaks of ammonium ferric sulfate disappear due to its decomposition. When the roasting temperature rises to 500°C, the diffraction peaks of $NaMgFe(SO_4)_3$ appear, indicating that the sodium sulfate has reacted with lizardite and talc. The diffraction peaks of $Na_3Fe(SO_4)_3{\cdot}3H_2O$ disappear because it has lost the crystal water to transform into $Na_3Fe(SO_4)_3$. The diffraction peaks of ammonium ferric sulfate disappear, indicating that it has been decomposed completely, partially being converted to $Na_3Fe(SO_4)_3$, and partially being decomposed into ferric oxide which is not shown by XRD because of its small amount.

Roasting Process Kinetics Analysis

The roasting process of low-grade nickel sulfide ore with ammonium sulfate and sodium sulfate contains liquid–solid and gas–solid reactions, which can be analyzed with the shrinking core model (SCM).[20] The chemical reactions can be expressed as Eqs. 3 and 4.

$$A_{(s)} + B_{(l)} \rightarrow C_{(s)} + D_{(g)} \tag{3}$$

$$A_{(s)} + D_{(g)} \rightarrow C_{(s)} \tag{4}$$

where A, B, C and D represent raw ore particles, molten chemical agents including ammonium sulfate and sodium sulfate, solid products and gas products.

In SCM, the roasting process consists of five steps as follows:

(a) The diffusion of reactants through the gas film and liquid film to the surface of the solid product;
(b) The diffusion of the reactants through the solid product layer to the reaction interface;
(c) A chemical reaction between the reactants and the raw ore at the interface;
(d) The diffusion of the product from the reaction interface through the product layer;
(e) The diffusion of the product from the boundary layer.

Steps (a) and (e) are collectively referred to as the external diffusion link, Steps (b) and (d) are collectively referred to as the internal diffusion link. The roasting process can be divided into three links: external diffusion, internal diffusion and chemical reaction. The overall rate of the roasting process depends on the slowest link, called the restrictive link. The reaction model of the roasting process is shown in Fig. 5f.

According to SCM, the integral rate equations for external diffusion, internal diffusion and the chemical reaction on the surface can be expressed as $1-(1-x)^{2/3} = k_l t$, $1+2(1-x)-3(1-x)^{2/3} = k_d t$, and $1-(1-x)^{1/3} = k_r t$, respectively,[21,22] where x is the conversion of metals, k_l is the apparent rate constant for external diffusion, k_d is the internal diffusion rate constant, k_r is the apparent rate constant for the surface chemical reaction and t is the roasting time.

The experimental data collected at different temperatures are treated using the above three equations. It is found that the experimental data before reaching reaction equilibrium have the best linear relationship with the equation $1+2(1-x)-3(1-x)^{2/3}$, presenting the internal diffusion controlled model as suitable for this roasting process. The linear relationship between $1+2(1-x)-3(1-x)^{2/3}$ and roasting time (t) for different metals is shown in Fig. 6a–d.

According to the Arrhenius equation, $k_d = k_0 \exp(-E_a/RT)$, a plot of $\ln k_d$ versus $1/T$ for different metals are straight lines with a slope of $-E_a/R$ and an intercept of $\ln k_0$, as seen in Fig. 6e. The apparent activation energy and rate constant for different metals were calculated as 5.03×10^{-2} min^{-1} (Ni), 14.51×10^{-2} min^{-1} (Cu), 5.50×10^{-2} min^{-1} (Fe) and 18.63×10^{-2} min^{-1} (Mg), respectively. The increase of the temperature has a slight effect on the diffusion rate, but a significant effect on the chemical reaction rate. The activation energy of a diffusion-controlled process is typically below 12 kJ mol^{-1}, while, for a chemical reaction-controlled process, the value is usually higher than 40 kJ mol^{-1}.[23,24] The apparent activation energy of different metal transformations was calculated as 12.06 kJ mol^{-1} (Ni), 18.95 kJ mol^{-1} (Cu), 15.15 kJ mol^{-1} (Fe) and 23.93 kJ mol^{-1} (Mg), respectively. These values show that the metal conversion rate is more dependent on the internal diffusion than the chemical reactions, and the closely bonded surface of the calcined clinker in Fig. 4c also shows that the formed product layer hinders the mass transfer inside the system and supports that the low-temperature roasting process is controlled by internal diffusion. The kinetics equation of various metal conversions can be expressed as follows:

$$\text{For Ni, } 1+2(1-x)-3(1-x)^{2/3} = 5.03 \times 10^{-2} \cdot \exp(-12.06/RT) \cdot t \tag{5}$$

$$\text{For Cu, } 1+2(1-x)-3(1-x)^{2/3} = 14.51 \times 10^{-2} \cdot \exp(-18.95/RT) \cdot t \tag{6}$$

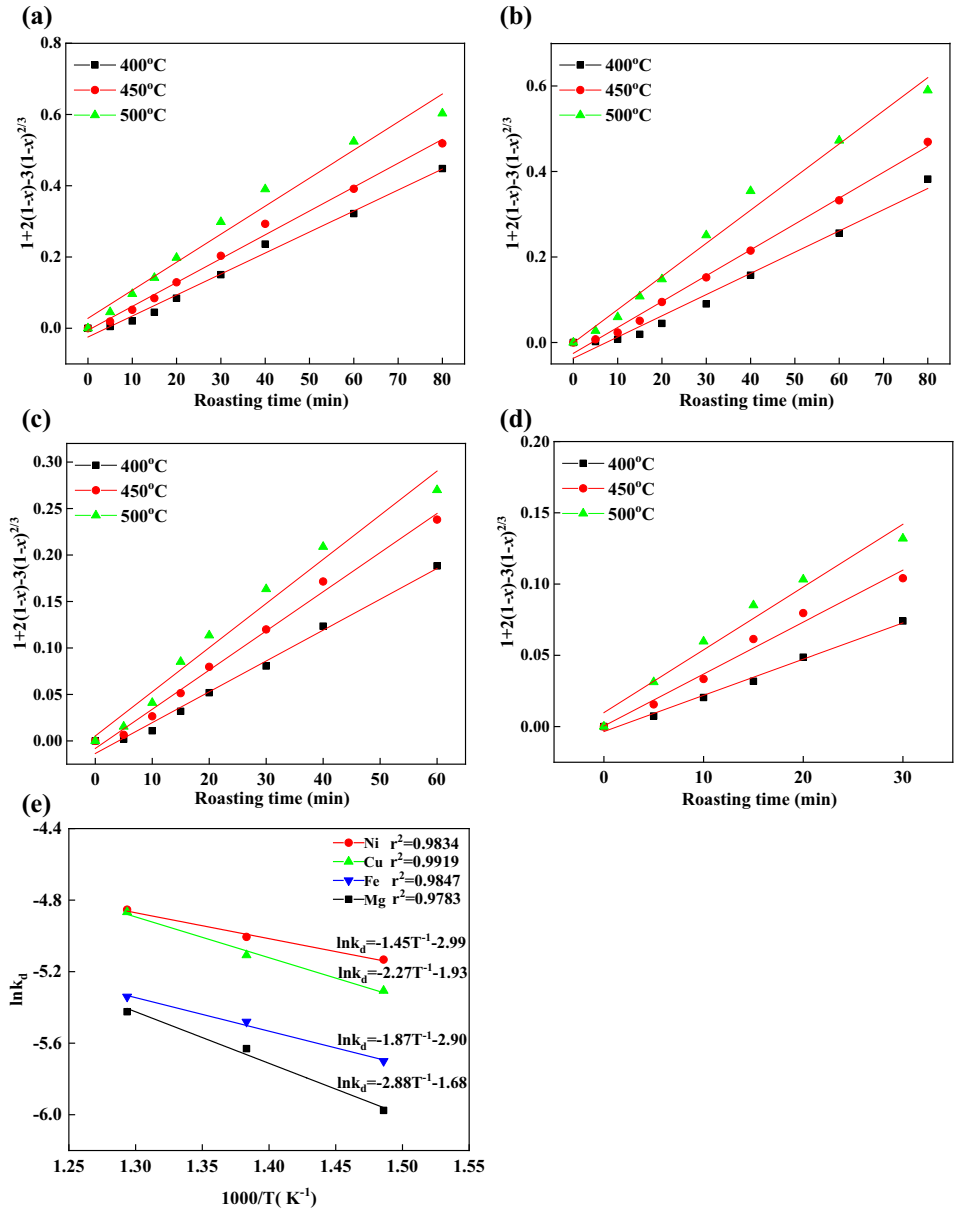

Fig. 6. Plots of $1 + 2(1 - x) - 3(1 - x)^{2/3}$ versus roasting time t at different roasting temperatures, (a) Ni; (b) Cu; (c) Fe; (d):Mg and (e) Arrhenius plot of the roasting process of low-grade nickel sulfide ore.

$$\text{For Fe, } 1 + 2(1-x) - 3(1-x)^{2/3} = 5.50 \times 10^{-2} \cdot \exp(-15.15/RT) \cdot t \quad (7)$$

$$\text{For Mg, } 1 + 2(1-x) - 3(1-x)^{2/3} = 18.63 \times 10^{-2} \cdot \exp(-23.93/RT) \cdot t \quad (8)$$

Iron Removal Process

Selective Decomposition

In the low-temperature roasting process, part of the iron and magnesium is converted into soluble metal double salts, entering the solution together with nickel and copper by water leaching. In order to reduce the difficulty of subsequent separation, the selective decomposition process was carried out to convert iron-containing sulfates into water-insoluble Fe_2O_3 based on the difference in thermal stability of metal sulfates,[25,26] and the effect of roasting temperature on metal conversions was investigated when the roasting time is 2 h. The raw material used in this process was the roasting clinkers obtained at the roasting temperature of 450°C, the roasting time of 120 min, MR of 1:0.4:3.5 and the ore particle size of − 140 + 160 mesh.

It can be seen from Fig. 7a that the conversion of nickel increases slightly with the increase of

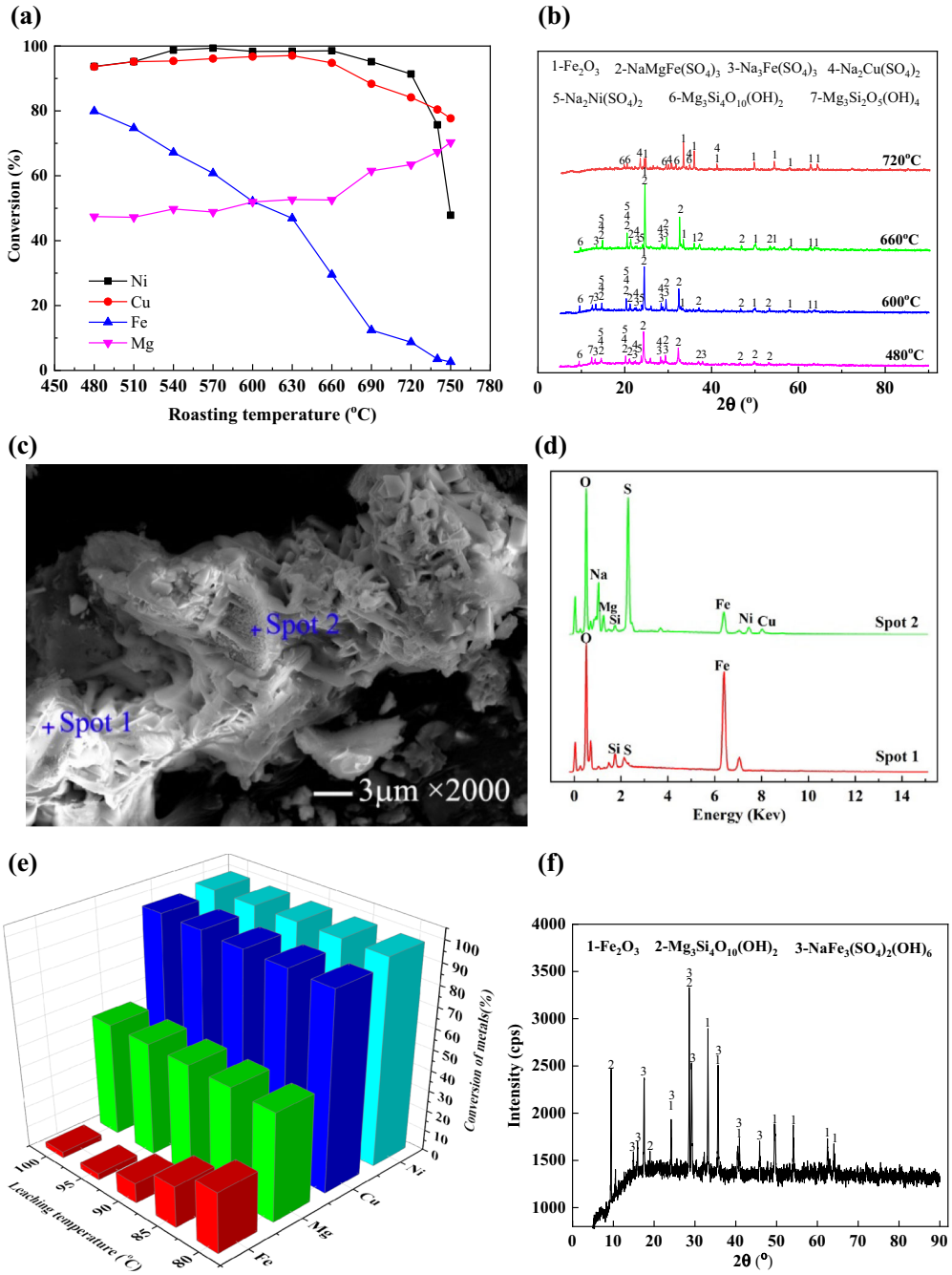

Fig. 7. The effect of roasting temperature (a) and leaching temperature (e) on the conversion of metals; XRD patterns of the clinkers (b), SEM images (c) and EDS analysis (d) of clinker; XRD pattern of the leaching residue (f).

temperature, and reach a maximum value of 98.54% at 660°C, which is 4.85% higher than that at 450°C. As the temperature continues to increase, the conversion of nickel first slowly decreases by 7.2% (from 660°C to 720°C) and then rapidly decreases by 43.5% (from 720°C to 750°C). The conversion of copper slightly increases with the increase of temperature, reaching a maximum of 97.05% at 630°C, and then decreases gradually to 77.7% with increase of temperature to 750°C. Magnesium conversion increases with the increase of roasting temperature and reaches 70.32% at 750°C. A significant decrease of iron conversion can be caused by increasing the roasting temperature, the value of which is reduced by 77.33% at 750°C. In order to avoid the loss of nickel and copper, it is appropriate to control the roasting temperature at 660°C, when the conversion of copper and iron is 94.81% and 29.5%, respectively, and the iron removal rate can reach 61.8%.

The XRD pattern of Fig. 7b shows that, when the roasting temperature is 600°C, the obvious diffraction peaks of ferric oxide appear, indicating that a

large amount of iron-containing double salts has been decomposed. When the temperature rises to 640°C, the diffraction peaks of the lizardite disappear. This means that lizardite has been converted into a soluble magnesium salt due to an increase in its reaction activity by elevating the roasting temperature. When the temperature is higher than 600°C, a part of $Na_2Cu(SO_4)_2$ has been decomposed, and the decomposition rate is slower than its formation rate. At 630°C, the formation rate of $Na_2Cu(SO_4)_2$ reaches the maximum, after which the decomposition rate of $Na_2Cu(SO_4)_2$ is faster than its formation rate, and causing a decrease copper conversion. When the temperature is 660°C, a part of $Na_2Ni(SO_4)_2$ is decomposed to cause a small decrease of nickel conversion. When the temperature is increased to 720°C, the diffraction peaks of $Na_2Ni(SO_4)_2$ disappear, indicating that a large amount has decomposed to cause a sharp decrease of nickel conversion. Some diffraction peaks of $Na_2Cu(SO_4)_2$ weaken or disappear, demonstrating the decomposition of $Na_2Cu(SO_4)_2$ Compared with the decomposition of $Na_2Ni(SO_4)_2$, the decomposition rate of the $Na_2Cu(SO_4)_2$ is slow, and the decomposition amount is small. The diffraction peaks of the iron-containing double salts also disappear at this temperature, showing that it is close to decomposing completely.

The morphology of the selective decomposed clinker observed by SEM in Fig. 7c shows that the clinker is in a honeycomb or a block shape. In order to determine the difference between the two types, their components were analyzed by EDS. The results in Fig. 7d show that the blocky clinker mainly contains O and Fe elements, indicating that its main component is ferric oxide (Spot 1). The compositions of the honeycomb clicker are mainly O, Na, S, Fe, Ni, and Cu elements indicating it mainly contains metal-sodium double salts (Spot 2). The results are consistent with the XRD analysis in Fig. 7b.

Elevating Leaching Temperature

The increase of leaching temperature can accelerate the precipitation rate of iron ions. Thus, the selective decomposed clinker was leached at a temperature higher than 80°C to obtain the appropriate temperature condition for iron removal. The results in Fig. 7e show that the increase of leaching temperature causes a slight increase of nickel, copper and magnesium conversion, but a significant decrease of iron conversion. When the leaching temperature is higher than 95°C, the iron removal rate is more than 34.15%, and the conversion of nickel and copper is greater than 99.13% and 96.74%, respectively. Through a two-step process of selective decomposition and elevating the leaching temperature, the total iron removal rate is greater than 95.95%, and the concentration of iron ions in the leaching solution is lower than 0.036 mol/L. The remaining leachate is mainly a solution containing copper, nickel and magnesium ions, and the separation of the metals can be achieved by first extracting the copper and then precipitating the nickel. However, this part of the research is not within the scope of this article.

The XRD patterns in Fig. 7f show that the main phase in the leaching residue is iron oxide, talc and natrojarosite. Compared with the pattern of 660°C in Fig. 7b, the diffraction peaks of the double salts containing nickel, copper, iron and magnesium disappear, which is mainly attributed to them being dissolved by water into solution. The diffraction peaks of natrojarosite appear due to the precipitation of iron ions during the leaching process. The talc in the ore is not completely reacted, so it remains in the leaching residue.

CONCLUSION

A low-temperature roasting, selective decomposition and water-leaching process was proposed to treat Jinchuan low-grade nickel sulfide ore with highly alkaline gangue to simultaneously extract copper and nickel. When the roasting temperature is 450°C, the roasting time is 120 min, MR is 1:0.4:3.5, the ore particle size is − 140 + 160 mesh, the selective decomposition temperature is 660°C and the leaching temperature is 95°C, more than 99.13% Ni and 96.74% Cu can be extracted, and 95.95% impurity iron can be effectively removed, while the iron concentration in the leaching solution is lower than 0.036 mol/L. In the low-temperature roasting process, the metal sulfides can be transformed into the metallic ammonium sulfate salts, part of which can further react with sodium sulfate to yield metal–sodium double salts. Ammonium ferric sulfate, ferric sulfate and iron–sodium double salt can be decomposed by selective roasting to produce ferric oxide, and iron ions entering the solution can be transformed into natrojarosite precipitation in the water-leaching process.

Kinetics analysis shows that the low-temperature roasting process of low-grade nickel sulfide ore is controlled by the internal diffusion of the shrinking core model. The activation energy of Ni, Cu, Fe and Mg was determined to be 12.06 kJ mol^{-1}, 18.95 kJ mol^{-1}, 15.15 kJ mol^{-1}, and 23.93 kJ mol^{-1}, respectively, and the general kinetics equations of various metals conversion can be expressed as: $1 + 2(1 - x) - 3(1 - x)^{2/3} = k_0 \exp(-E_a/RT) \cdot t$.

ACKNOWLEDGEMENTS

This study was supported by the National Basic Research Program of China (Grant 2014CB643405), National Natural Science Foundation of China (Grant 51204036) and the Fundamental Research Funds for the Central Universities (No. N182304016).

REFERENCES

1. C. Wang, B. Wei, M. Zhou, D. Minh, and L. Qi, *J. Asian Earth Sci.* 154, 162 (2018).
2. Y. Liu, W. Li, X. Lü, Y. Liu, B. Ruan, and X. Liu, *Ore Geol. Rev.* 91, 419 (2017).
3. M. Gericke and Y. Govender, *Miner. Eng.* 24, 1106 (2011).
4. K. Zhao, G. Gu, H. Wang, C. Wang, X. Wang, and C. Luo, *Int. J. Miner. Process.* 141, 68 (2015).
5. G.D. Senior and S.A. Thomas, *Int. J. Miner. Process.* 78, 49 (2005).
6. W. Chimonyo, K. Corin, J. Wiese, and C. O'Connor, *Miner. Eng.* 110, 57 (2017).
7. K. Zhao, G. Gu, C. Wang, X. Rao, X. Wang, and X. Xiong, *Miner. Eng.* 77, 99 (2015).
8. A.M. Amer, *Hydrometallurgy* 58, 251 (2000).
9. Y. Xie, Y. Xu, L. Yan, and R. Yang, *Hydrometallurgy* 80, 54 (2005).
10. W. Qin, S. Zhen, Z. Yan, M. Campbell, J. Wang, K. Liu, and Y. Zhang, *Hydrometallurgy* 98, 58 (2009).
11. S. Zhen, Z. Yan, Y. Zhang, J. Wang, M. Campbell, and W. Qin, *Hydrometallurgy* 96, 337 (2009).
12. C. Yang, W. Qin, S. Lai, J. Wang, Y. Zhang, F. Jiao, L. Ren, T. Zhuang, and Z. Chang, *Hydrometallurgy* 106, 32 (2011).
13. H. Li and J. Ke, *Hydrometallurgy* 61, 151 (2001).
14. H. Li and J. Ke, *Miner. Eng.* 14, 113 (2001).
15. B. Xu, Y. Yang, Q. Li, T. Jiang, and G. Li, *Hydrometallurgy* 159, 87 (2016).
16. G. Zhang, D. Luo, C. Deng, L. Lv, B. Liang, and C. Li, *J. Alloys Compd.* 742, 504 (2018).
17. J. Li, Z. Chen, B. Shen, Z. Xu, and Y. Zhang, *J. Clean. Prod.* 140, 1148 (2017).
18. X. Liu, Y. Feng, H. Li, Z. Yang, and Z. Cai, *Int. J. Miner. Metall. Mater.* 19, 377 (2012).
19. F. Cui, W. Mu, S. Wang, H. Xin, Q. Xu, Y. Zhai, and S. Luo, *Miner. Eng.* 123, 104 (2018).
20. O. Levenspiel, *Ind. Eng. Chem. Res.* 38, 4140 (1999).
21. Z. Yang, H.Y. Li, X.C. Yin, Z.M. Yan, X.M. Yan, and B. Xie, *Int. J. Miner. Process.* 133, 105 (2014).
22. C. Wen, *Ind. Eng. Chem.* 60, 34 (1968).
23. E. Kavcı, T. Çalban, S. Çolak, and S. Kuşlu, *J. Ind. Eng. Chem.* 20, 2625 (2014).
24. M. Ashraf, Z.I. Zafar, and T.M. Ansari, *Hydrometallurgy* 80, 286 (2005).
25. R.V. Siriwardane, J.A.P. Jr, E.P. Fisher, M.S. Shen, and A.L. Miltz, *Appl. Surf. Sci.* 152, 219 (1999).
26. H. Tagawa, *Thermochim. Acta* 80, 23 (1984).

Publisher's Note Springer Nature remains neutral with regard to jurisdictional claims in published maps and institutional affiliations.